

# Improving Robustness and Efficiency in Active Learning with Contrastive Loss

Ranganath Krishnan<sup>\*</sup>, Nilesh Ahuja<sup>\*</sup>, Alok Sinha<sup>†</sup>, Mahesh Subedar<sup>\*</sup>, Omesh Tickoo<sup>\*</sup>, Ravi Iyer<sup>\*</sup>

<sup>\*</sup> Intel Labs, Hillsboro, USA

<sup>†</sup> Intel Corporation, Bangalore, India

## Abstract

This paper introduces supervised contrastive active learning (SCAL) by leveraging the contrastive loss for active learning in a supervised setting. We propose efficient query strategies in active learning to select unbiased and informative data samples of diverse feature representations. We demonstrate our proposed method reduces sampling bias, achieves state-of-the-art accuracy and model calibration in an active learning setup with the query computation 11x faster than CoreSet and 26x faster than Bayesian active learning by disagreement. Our method yields well-calibrated models even with imbalanced datasets. We also evaluate robustness to dataset shift and out-of-distribution in active learning setup and demonstrate our proposed SCAL method outperforms high performing compute-intensive methods by a bigger margin (average 8.9% higher AUROC for out-of-distribution detection and average 7.2% lower ECE under dataset shift).

## 1 Introduction

Deep learning relies on a large amount of labeled data for training the models. Data annotation is often very expensive and time-consuming. It is challenging to obtain labels for large-scale datasets in complex tasks such as medical diagnostics (Irvin et al. 2019) that require specific expertise for data labeling, and semantic segmentation (Cordts et al. 2016) requiring pixel-wise labeling. Active learning (Settles 2009; Lewis and Gale 1994) is a promising solution that allows the model to choose the most informative data samples from which it can learn while requesting a human annotator to label the carefully selected data based on some query strategy. Deep active learning has been widely studied recently (Gal, Islam, and Ghahramani 2017; Shen et al. 2018; Sener and Savarese 2018; Beluch et al. 2018; Ducoffe and Precioso 2018; Yoo and Kweon 2019; Kirsch, Van Amersfoort, and Gal 2019), but there remain many open questions which we enumerate below.

First, existing research has mainly focused on improving the model accuracy as samples are acquired, but accuracy alone is not indicative of the robustness of the trained network. It has been shown that once deep neural networks are trained, they face challenges in real-world conditions such as dataset shift and out-of-distribution data (Ovadia et al.

2019; Krishnan and Tickoo 2020). Dataset shifts (Quionero-Candela et al. 2009) arise due to the non-stationary environments in the real-world as the observed data evolve from training data distribution and models can encounter novel scenarios (Hendrycks and Gimpel 2017). Models should be well-calibrated and robust under such shifts in order to be deployed in safety-critical applications. This is particularly important in an active-learning setting since we need to ensure that the model remains robust despite being trained with fewer samples.

Moreover, in real-world applications, the collected datasets often follow long-tailed distribution where the number of samples for different classes are highly imbalanced (Liu et al. 2019). We show that models trained with existing active-learning methods show poor robustness when the datasets are highly imbalanced. Even when the datasets are balanced, active learning introduces sampling bias (Dasgupta and Hsu 2008; Dasgupta 2011; Farquhar, Gal, and Rainforth 2020) owing to the heuristic nature of sample selection. Sampling bias in deep neural network training can cause undesired behavior with respect to fairness, robustness and trustworthiness when deployed in real-world situations (Buolamwini and Gebru 2018; Bhatt et al. 2021).

We investigate and address these problems in this paper, and propose an active-learning method based on contrastive learning. Recent advancements in contrastive learning (Chen et al. 2020a,b; He et al. 2020; Chen et al. 2020c) have resulted in state-of-the-art performance in unsupervised representation learning. We extend the contrastive loss to active learning in a supervised setting to leverage the powerful feature representations. We further present an unbiased sample-selection strategy that leverages the feature representations from the neural network. The strategy is devised to select data samples with diverse features while maintaining an equal representation of samples from each class in order to mitigate the sampling bias. Unlike other sample-selection methods such as CoreSet approach (Sener and Savarese 2018) which results in very high query time at every active learning iteration (Shui et al. 2020), our method is fast and computationally inexpensive.

With these innovations – use of contrastive learning, and an unbiased and efficient sample-selection strategy – we show that our method outperforms existing methods in terms of model robustness while achieving accuracy at-par or better

than existing methods. We compare our methods with high-performing active learning methods including CoreSet (Sener and Savarese 2018), Learning Loss (Yoo and Kweon 2019) and Bayesian active learning by disagreement (BALD) (Gal, Islam, and Ghahramani 2017). Our method is 26x faster than BALD and 11x faster than CoreSet in query computation, while achieving state-of-the-accuracy in both imbalanced and balanced datasets scenario, and retaining expected calibration error (ECE) within average of only 0.8% higher than BALD. It also significantly outperforms all the methods by a bigger margin in robustness to distributional shift (average 8.9% higher AUROC for out-of-distribution detection and average 7.2% lower ECE under dataset shift).

In summary, our **main contributions** include:

- We propose supervised contrastive active learning (SCAL) by leveraging the contrastive loss and the query strategies based on the feature similarity (*featuresim*) and PCA-based feature-reconstruction errors (*fre*) of feature distributions
- We evaluate the model calibration and robustness in active learning setup, demonstrating our method yields well-calibrated models and clearly outperforms existing methods in robustness to dataset shift and out-of-distribution data.
- We demonstrate the proposed method is computationally efficient in selecting diverse and informative data samples in active learning, reduces the sampling bias and improves active learning performance in both balanced and imbalanced dataset scenarios.

## 2 Problem setup and Background

Active learning aims to learn from a small set of informative data samples, which are acquired from a huge unlabeled dataset, thus minimizing the data annotation cost. The acquired data samples are labeled by an oracle (e.g. human annotator), which is used for training the model. In this framework, the models are allowed to select the data from which they can learn based on a query strategy. The query strategy evaluates the informativeness of data samples; some of the commonly used strategies include the uncertainty-based approach (Lewis and Gale 1994; Tong and Koller 2001) and diversity-based approach (Brinker 2003). For example, the data samples with higher uncertainty estimates are considered to be most useful in uncertainty-based query strategy. We refer to (Settles 2009) for an overview of earlier works in active learning.

**Problem formulation:** Let  $f_w(\cdot)$  represent a deep neural network with weights  $w$  that is to be trained for a multi-class classification problem with a limited data labeling budget. Let  $\mathcal{D}_U = \{x_u\}_{u=1}^N$  represent an initial large pool of unlabeled data. Initially a small set of  $M$  samples are randomly sampled from  $\mathcal{D}_U$  and annotated by an oracle (human annotator) to obtain initial labeled set  $\mathcal{D}_L^1 = \{(x_\ell, y_\ell)\}_{\ell=1}^M$ , where  $y_\ell \in \{c_1, c_2, \dots, c_k\}$  is the ground-truth class label with  $K$ -classes. The labeled  $M$  samples are removed from the unlabeled pool and model is trained with  $\mathcal{D}_L^1$ . The next batch of  $M$  samples for the next training iteration of the

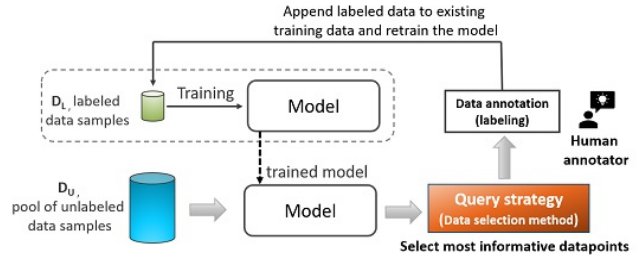


Figure 1: Active Learning setup

active-learning are chosen from the remaining unlabeled data  $\mathcal{D}_U^1 = \mathcal{D}_U \setminus \mathcal{D}_L^1$ . These are chosen based on an acquisition function  $\mathcal{Q}(\mathcal{D}, f_w, \mathcal{S})$  that evaluates the samples from dataset  $\mathcal{D}$  on the network  $f_w$  and determines the indices  $I_M$  of the  $M$  samples that yield the highest scores on a scoring function  $\mathcal{S}$ .  $\mathcal{S}$  depends on the particular method used and typically indicates the uncertainty in the prediction of a sample from  $f_w$ . The query function  $\mathcal{Q}$  returns, therefore, the most informative samples for the next active learning iteration. These samples are annotated by an oracle and added to existing labeled set  $\mathcal{D}_L^1$  to create  $\mathcal{D}_L^2 = \mathcal{D}_L^1 \cup \{(x_\ell, y_\ell)\}_{\ell \in I_M}$ , and simultaneously are removed from the unlabeled set to obtain  $\mathcal{D}_U^2 = \mathcal{D}_U \setminus \mathcal{D}_L^2$ . Thus, a sequence of  $[\mathcal{D}_L^1, \mathcal{D}_L^2, \mathcal{D}_L^3, \dots]$  labeled sets of size  $[M, 2M, 3M, \dots]$  samples and corresponding trained models  $[f_w^1, f_w^2, f_w^3, \dots]$  are obtained from every iteration of active learning. This cycle is repeated until a desired model performance is achieved or until the query budget is reached as shown in Fig. 1.

**Contrastive learning** Contrastive learning (Chen et al. 2020a,b; He et al. 2020; Chen et al. 2020c) requires positive and negative samples in a mini-batch to bring the positive samples closer in the feature space while pushing the negative samples further apart. In the self-supervised setting, positive samples are selected by applying data augmentation and the rest of the samples are assumed to be negative examples. Khosla et al. propose a generalization to contrastive loss by extending to a fully-supervised learning setting by leveraging the label information.

To the best of our knowledge, the work presented in this paper is the first to apply the contrastive learning method in active learning setup and also the first work to evaluate the robustness to distributional shift of models resulting from different query strategies in active learning setting.

Our motivation is to combine the benefits of uncertainty and diversity-based approaches, while keep the query method computationally less expensive. We achieve this by leveraging the well-clustered feature representations learnt from contrastive loss in supervised setting and proposing query functions that are simple, computationally less expensive and yet efficient to select diverse and most informative samples. Our unbiased query strategy is based on the per-cluster feature similarity in the feature embedding space.

### 3 Proposed Method

In this section, we present our proposed method supervised contrastive active learning (SCAL) with the query strategies based on the *feature similarity (featuresim)* and *feature reconstruction error (fre)* scores. We follow the problem formulation and notations described in Section 2.

#### 3.1 Supervised Contrastive Active Learning

We extend the contrastive loss proposed in (Khosla et al. 2020) to active learning in a supervised setting. At every active learning iteration, the model is trained with newly acquired labeled data using the loss function given by Equation (1).

$$\mathcal{L}_{con} = \sum_{i \in I} \frac{-1}{|P(i)|} \sum_{p \in P(i)} \log \frac{\exp(\mathbf{z}_i \cdot \mathbf{z}_p / T)}{\sum_{a \in A(i)} \exp(\mathbf{z}_i \cdot \mathbf{z}_a / T)} \quad (1)$$

$\mathbf{z}$  is the feature from the neural network,  $T$  is scalar temperature parameter,  $i \in I$  is the index of sample in augmented batch,  $P(i)$  is the set of all positives corresponding to the index  $i$  and  $|P(i)|$  is its cardinality, and  $A(i) \in I \setminus \{i\}$ . The contrastive loss helps in learning better feature representations as it pulls together clusters of samples from the same class and pushes apart clusters of samples from different classes in the feature space (see, for example, the clusters in Fig. 2).

We take advantage of this class-based clustering to propose a strategy for selecting a set of diverse, unbiased and informative samples from the unlabeled pool. Suppose a batch of  $M$  samples has to be selected from the unlabeled set as described in Section 2. Ideally, we would like to choose an equal number of samples from each of the  $K$  classes. Since true class-labels,  $y$  are not available for the samples in the unlabeled pool, we use the predicted class labels,  $\hat{y}$ . If  $\hat{y} = c_k$ , then we calculate a score between the observed feature and cluster of previously labeled features from class  $k$  only. This allows us to select  $M/K$  samples per predicted class which leads to a balanced sample selection, as demonstrated empirically in subsection 4.3. Within such a scheme, the use of simple and inexpensive distance-based scores in the feature space suffices for sample-selection without the need for expensive algorithms such as k-Center-Greedy used in Coreset. Specifically, we propose two simple and inexpensive scoring functions: a feature similarity (*featuresim*) score, which measures the similarity between a feature and a cluster, and a feature reconstruction error (*fre*) score, which measures the distance of a feature from a cluster. Both of these are described next. We refer to this method as supervised contrastive active learning (SCAL).

**SCAL (*featuresim*)** As contrastive loss minimizes cosine similarity between similar samples, it tends to increase the norm of the representation. The *featuresim* score leverages the norm of the feature representation and cosine similarity between the sample from unlabeled pool and corresponding training features embedding belonging to the same class as the prediction. Similar properties of contrastive loss have been leveraged in (Tack et al. 2020) for novelty detection but without the importance of class-conditional or per-cluster

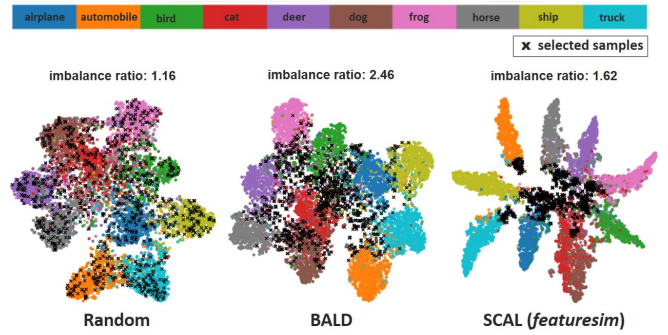


Figure 2: tSNE embedding of CIFAR10/ResNet-18 showing selected samples with different query methods at fourth iteration in active learning. Our proposed SCAL method selects balanced, diverse and informative samples (samples in-between clusters and from edge of clusters) from each class. Imbalance ratio indicates ratio of samples from most frequent and least frequent class.

feature representation. The query function  $\mathcal{Q}$  is intended to obtain  $M/K$  samples from each cluster in feature embedding space based on the feature similarity score as given by Eq. (2). Here,  $l$  is an index over the labeled set and we only consider those samples for which the true label  $y_l = c_k$ .

$$\mathcal{S} \triangleq score(x) := \max_{\ell} \frac{z(x_{\ell} | y_{\ell} = c_k)}{\|z(x_{\ell} | y_{\ell} = c_k)\|} \cdot z(x | \hat{y} = c_k) \quad (2)$$

We refer to this as SCAL (*featuresim*), where the query function selects the samples with the least *featuresim* scores at each iteration in active learning.

**SCAL (*fre*)** The *feature reconstruction error* score measures the distance between an observed feature and the subspace spanned by the cluster of features from a specific class. To calculate this, we adopt and extend the approach proposed in Ahuja et al. (2019) for detecting out-of-distribution samples. That approach involved fitting class-conditional probability distributions to the deep-features,  $z$ , of a DNN and using the log-likelihood scores under those distributions to discriminate in-distribution samples (high likelihood) from OOD samples (low likelihood). Prior to learning distribution, the dimension of the feature space was reduced by applying a set of class-conditional PCA (principal component analysis) transforms,  $\{\mathcal{T}_k\}_{k=1}^K$ . Instead of using the log-likelihood score as originally proposed, we instead use a simpler score, which is the norm of the difference between the original feature vector and the pre-image of its corresponding reduced embedding:

$$\mathcal{S} \triangleq FRE(z | y = c_k) = \|z - (\mathcal{T}_k^{\dagger} \circ \mathcal{T}_k)(z)\|_2. \quad (3)$$

Here,  $\mathcal{T}_k$ , is the forward PCA transformation, and  $\mathcal{T}_k^{\dagger}$  is its Moore-Penrose pseudo-inverse. Intuitively, we wish to select samples that are most distant from the reduced-dimension PCA subspace. Note that this circumvents the need for modeling distributions, thereby simplifying the process.

## 4 Experiments and Results

### 4.1 Experimental setup

We perform a thorough empirical evaluation on image classification tasks with balanced and imbalanced datasets.

We use CIFAR-10 (Krizhevsky et al. 2009) for balanced, long-tailed Imbalanced-CIFAR10 (Cao et al. 2019) and Street View House Numbers (SVHN) (Netzer et al. 2011) for imbalanced setup (dataset details are provided in Appendix A). We use CIFAR10-C (Hendrycks and Dietterich 2018) to evaluate robustness of models derived from different query methods to distributional shift. CIFAR10-C comprises 80 variations of dataset shift resulting from 16 different types of image corruptions and perturbations at 5 different levels of intensities for each dataset shift type.

We compare our proposed SCAL(*featuresim*) and SCAL(*fre*) with the state-of-the-art methods including Learning loss (Yoo and Kweon 2019), CoreSet (Sener and Savarese 2018) and Bayesian active learning by disagreement (BALD) (Gal, Islam, and Ghahramani 2017) along with baseline Random and Entropy query methods. These query strategies are described in Appendix A.4.

We use ResNet-18 (He et al. 2016) model architecture for all the methods and datasets under study. We use the same hyperparameters for all the models for a fair comparison. The models are trained with the SGD optimizer with an initial learning rate of 0.1, the momentum of 0.9, and weight decay of 0.0005 for 200 epochs. The initial learning rate is multiplied by 0.1 at epoch 160. At each iteration in active learning, the models are trained with labeled samples acquired through the query strategy from respective methods. At the end of each active learning iteration, the models are evaluated with the labeled test set. We use these hyperparameters for all three datasets in our experiments. The implementation details are provided in Appendix A.3.

As in a typical active learning setup, we assume there are no labels available initially in the training set. The initial unlabeled set  $\mathcal{D}_U$  has 50K samples for CIFAR10, 14K samples for Imbalanced-CIFAR10 and 73.2K samples for SVHN. We set  $M = 1000$  for CIFAR10 and SVHN datasets, and  $M = 500$  for Imbalanced-CIFAR10. As described in Section 2, the model is trained iteratively with a sequence of labeled datasets  $[\mathcal{D}_L^1, \mathcal{D}_L^2, \dots]$ . Initially, we start with  $M$  labeled samples to train the model. At every iteration, we choose and annotate  $M$  additional samples according to the strategy described in Section 3. After every iteration, we evaluate with independent labeled test samples. For each method, we present the results for 10 iterations from 5 independent trials.

### 4.2 Evaluation metrics

We evaluate the models in active learning setup with various metrics\*. The model performance and efficiency of query strategy is evaluated using test accuracy ( $\uparrow$ ), sampling bias ( $\downarrow$ ) and query time ( $\downarrow$ ). Model calibration and robustness to dataset shift is evaluated using Expected calibration error (ECE) ( $\downarrow$ ) (Naeni, Cooper, and Hauskrecht 2015) and proper scoring rules including Negative log-likelihood (NLL)( $\downarrow$ ) and

\* Arrows next to each metric indicate lower( $\downarrow$ ) or higher( $\uparrow$ ) value is better.

Table 1: **Query time**  $\downarrow$  (unit relative to Entropy method as baseline) for computing the scores to select 1K most informative samples from a subset of 10K samples from the unlabeled pool at each iteration in active learning with ResNet-18/CIFAR-10.

QUERY METHOD	AVG. QUERY TIME UNIT $\downarrow$
ENTROPY	1.0
LEARNING LOSS	1.803
CORESET	15.181
BALD <sup>†</sup>	35.693
SCAL ( <i>fre</i> )	1.378
SCAL ( <i>featuresim</i> )	1.373

Brier score ( $\downarrow$ ) (Brier 1950). Robustness to out-of-distribution (OOD) is evaluated using *area under the receiver operating characteristic curve* (AUROC) ( $\uparrow$ ) (Davis and Goadrich 2006).

Sampling Bias measures the class imbalance in the acquired data. We propose the following score which measures the deviation from a balanced (uniform) distribution over the classes:

$$\text{Sampling Bias} = 1 - \frac{\mathcal{H}_{D_L}}{\mathcal{H}_{balanced}}. \quad (4)$$

Here,  $\mathcal{H}_{D_L}$ , is the entropy of the sample distribution over the labeled dataset defined as:

$$\mathcal{H}_{D_L} = - \sum_{k=1}^K \left( \frac{M_k}{M} \right) \log \left( \frac{M_k}{M} \right), \quad (5)$$

where  $M_k$  is the number of samples from class  $c_k$ , and  $M = \sum_k M_k$  is the total number of samples.  $\mathcal{H}_{balanced}$  is the entropy of a balanced sample distribution for which all  $M_k$  are equal. With this definition, sampling bias is always between 0 and 1, with 0 indicating no bias (perfectly balanced sample distribution) and 1 indicating a fully imbalanced distribution in which all samples belong to only one class and the other classes having no samples.

### 4.3 Results

**Accuracy and Query time:** Fig. 3 shows all the methods improve accuracy with the increase in training set size as samples are acquired and perform better than the random selection of samples. SCAL method outperforms in the imbalanced setup (Imbalanced-CIFAR10 and SVHN) and in the initial active learning iterations for balanced setup (CIFAR10), even with fewer training samples.

In Table 1, we compare the query time for all the methods to select 1k new training samples from a subset of 10k samples in the unlabeled pool of CIFAR10. For a fair comparison, these measurements are captured on the same compute machine and experimental settings for all the methods. The average query time is reported as a relative unit with Entropy method as the baseline. The query time measures the time needed to compute the respective scores for selecting the most informative samples. Table 1 shows that SCAL method

<sup>†</sup> 50 stochastic forward passes (Monte Carlo Dropout)

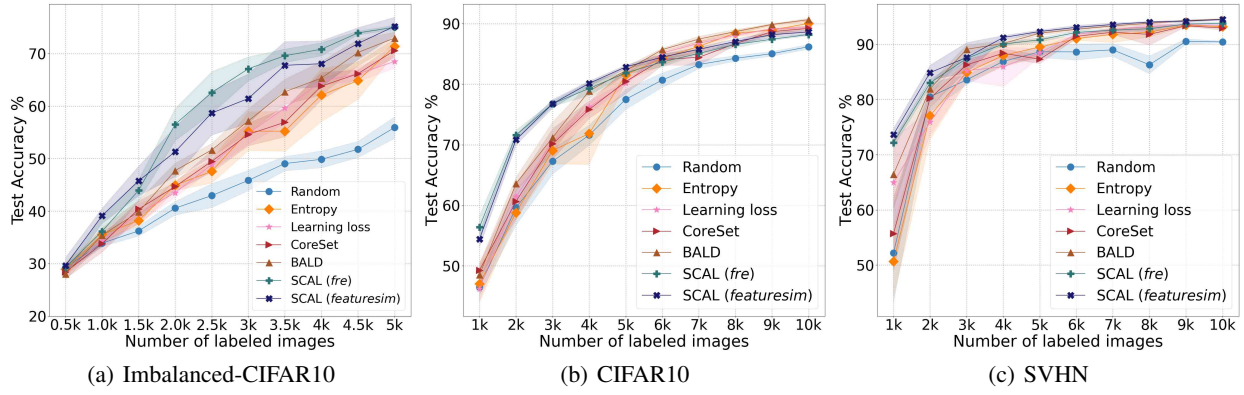


Figure 3: Test Accuracy  $\uparrow$  as a function of acquired data samples with different query methods in active learning for Imbalanced-CIFAR10, CIFAR10 and SVHN datasets. The shading for this and subsequent plot shows std-dev from 5 independent trials for each method. SCAL achieves accuracy comparable to other methods for balanced datasets (CIFAR10) and clearly outperforms on imbalanced datasets.

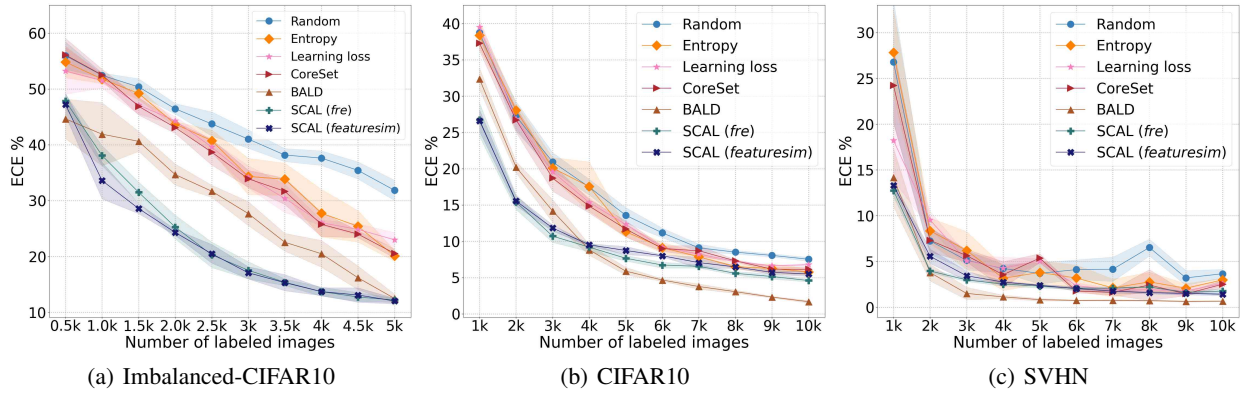


Figure 4: Expected Calibration Error (ECE)  $\downarrow$  as a function of acquired data samples with different query methods in active learning for Imbalanced-CIFAR10, CIFAR10 and SVHN datasets. Lower ECE is better, indicating the model is well-calibrated. SCAL yields lowest ECE on long-tailed Imbalanced-CIFAR-10 while BALD yields the lowest ECE for balanced datasets, but it is computationally expensive as noted in Table(1).

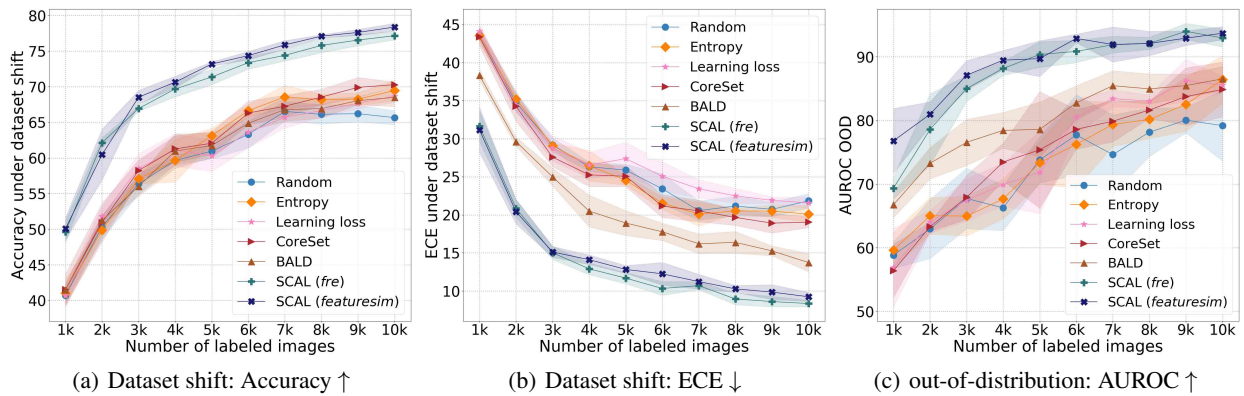


Figure 5: Robustness to dataset shift (CIFAR10-C with 16 different shift types) and out-of-distribution data (in-distribution: CIFAR-10, out-of-distribution (OOD): SVHN). (a) Accuracy under dataset shift: SCAL is more accurate even under dataset shift due to better learnt feature representation which are well clustered as shown in tSNE embedding in Fig. 7. (b) ECE on shifted data: SCAL yield reliable confidence under dataset shift as reflected by lower ECE. (c) AUROC of OOD detection shows SCAL outperforming existing methods.

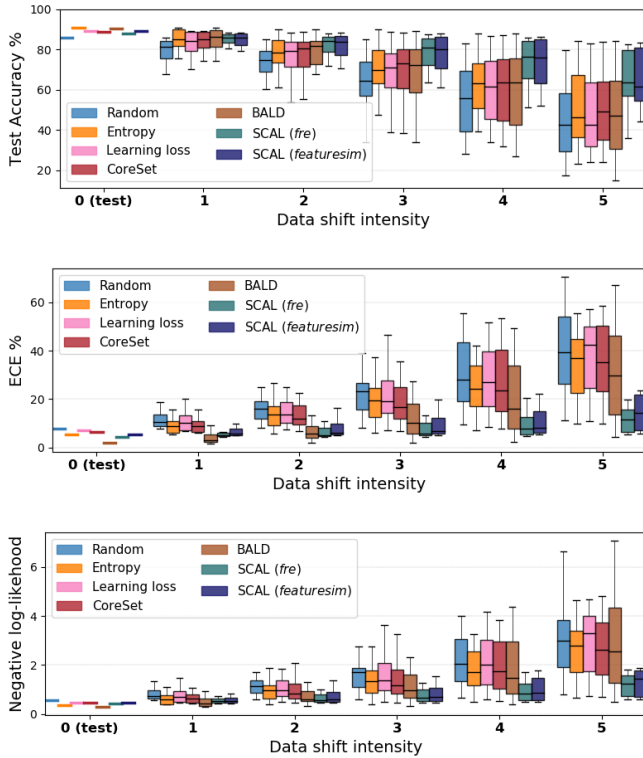


Figure 6: Robustness to dataset shift comparison of models derived with different query methods in active learning setting (10th iteration). Evaluation using Accuracy $\uparrow$ , ECE $\downarrow$  and Negative log-likelihood (NLL) $\downarrow$  on CIFAR10 under dataset shift at different levels of shift intensities (1-5). At each data shift intensity level, the boxplot summarizes the results across 16 different shift types showing the min, max and quartiles. Our proposed SCAL consistently yields higher accuracy, lower ECE and NLL even with increased dataset shift intensity, demonstrating better robustness compared to other high-performing methods.

using *featuresim* and *fre* scores is 26x faster than BALD and 11x faster than CoreSet.

**Model Calibration:** The models need to provide reliable, calibrated confidence measures in addition to providing accurate predictions, which is quantified with Expected Calibration Error (ECE) at every active learning iteration. Fig. 4 shows that SCAL yields lowest ECE on long-tailed imbalanced CIFAR10 while BALD provides lower ECE for fairly balanced datasets at the expense of significantly higher computational cost, attributed to multiple Monte Carlo stochastic forward passes during inference.

**Robustness to distributional shift:** We evaluate the robustness to dataset shift and out-of-distribution data for the models trained under active learning setting. The models need to be robust to distributional shift as the observed data may shift from the training data distribution in real-world.

**Dataset shift** We studied the robustness to dataset shift with CIFAR10 perturbed with 16 different shift types and

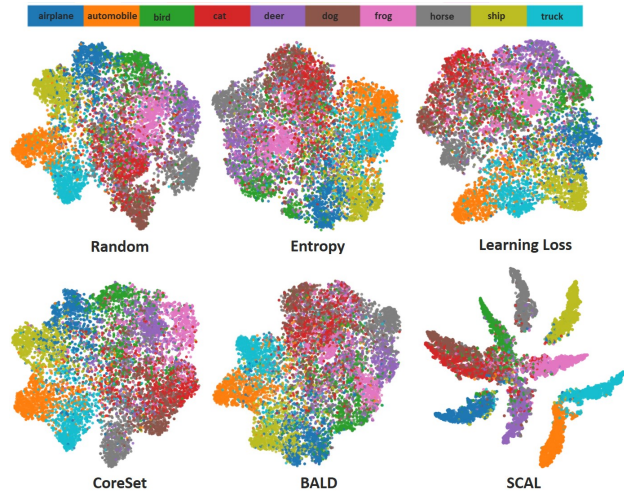


Figure 7: t-SNE of CIFAR10-C (dataset shift: Gaussian blur corruption, intensity level 3) feature distribution from models obtained with different query methods at fourth iteration in active learning setting. Note that the models are trained with clean CIFAR10.

5 different intensity levels for each datashift type (such as Gaussian blur, brightness, contrast, etc.) (Hendrycks and Dietterich 2018). Fig. 5 (a) & (b) shows the mean accuracy and ECE across 16 different shifts at level 3. SCAL method outperforms all other methods by a bigger margin by yielding higher test accuracy and lower calibration error demonstrating the robustness under dataset shift. The boxplots in Fig. 6 summarize the results across all shift types and intensity levels after final active learning iteration. Even at increased intensity of dataset shift, SCAL provides higher accuracy, lower ECE and NLL demonstrating robust and well-calibrated models in active learning setting. The superior robustness from SCAL method can be attributed to the powerful feature representations learnt from the selected samples. Fig. 7 shows the feature embeddings of SCAL method is well clustered and well separated between classes even under dataset shift, as compared to other methods.

Table 2: Robustness to distributional shift at 10th active learning iteration. OOD evaluation with SVHN and datashift evaluation with CIFAR10-C for models trained on CIFAR10.

Methods	AUROC $\uparrow$ (OOD det)	Accuracy $\uparrow$ (datashift)	ECE $\downarrow$ (datashift)
Random	79.18	65.65	21.84
Entropy	86.41	69.47	20.09
Learning Loss	85.55	68.67	21.57
CoreSet	84.85	70.28	19.04
BALD	86.53	68.50	13.73
SCAL ( <i>fre</i> )	<b>92.95</b>	<b>77.15</b>	<b>8.35</b>
SCAL ( <i>featuresim</i> )	<b>93.69</b>	<b>78.36</b>	<b>9.24</b>

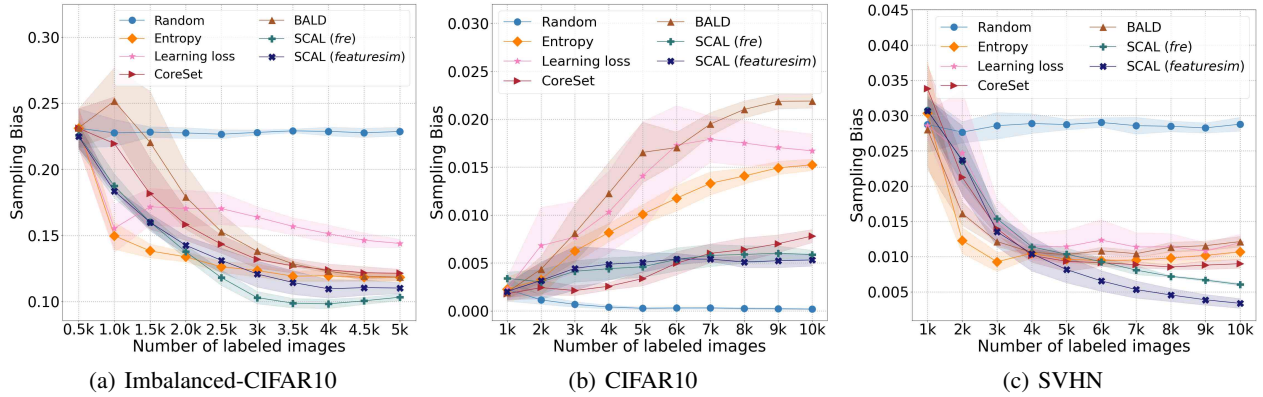


Figure 8: Sampling bias  $\downarrow$  evaluation of different query methods in active learning for Imbalanced-CIFAR10, CIFAR10 and SVHN datasets. The shading shows std-dev from 5 independent trials for each method. It is to be noted that Imbalanced-CIFAR10 and SVHN has an inherent bias in the dataset with significant imbalance in the number of classes, while CIFAR10 is balanced. SCAL has lower sampling bias learning from both balanced and imbalanced datasets.

**Out of distribution (OOD):** We compare the OOD detection performance for a model trained on CIFAR10 and evaluated on SVHN. This is a binary classification task of identifying if a test sample belongs to in- vs. out-of-distribution. For each of the methods, the same scoring function that was used to select the samples in active learning iteration is used to compute the AUROC for OOD detection. As shown in Fig. 5 (c), and in Table 2, SCAL method yields consistently higher AUROC compared to other state-of-the-arts methods.

**Sampling bias:** The plots shown in Fig. 8 demonstrate the sampling bias across classes in the acquired data. SCAL with *featuresim* and *fre* query strategy shows lower sampling bias at every active learning iteration. Imbalanced-CIFAR10 and SVHN are imbalanced datasets with inherent bias between classes, which is reflected in the random selection of the samples at every iteration. But, our proposed query methods help in reducing the sampling bias for both balanced and imbalanced datasets.

**Qualitative Analysis using tSNE:** We study the feature representations obtained from different methods with t-SNE (Van der Maaten and Hinton 2008) embeddings. Fig. 2 shows the feature embeddings from different methods at 4th iteration of the active learning. The plots visualize the data samples corresponding to 10 classes with 10 different colors. The samples shown with black markers are the most informative samples selected by the query strategies of corresponding methods. We notice that the features of SCAL method are well clustered even at 4th iteration and show lower class imbalance ratio (Cao et al. 2019). This signifies *featuresim* selected balanced samples yet diverse and informative samples (samples in-between clusters and from edge of clusters) from each clusters. Further qualitative analysis on sample selection exploration is presented in Appendix B.2.

**Ablation studies:** We performed an ablation study to understand the effect of proposed query functions *featuresim* and *fre*, and training the model with contrastive versus cross-entropy loss in active learning setting. We compared the query

methods including Random, Entropy, CoreSet, *featuresim* and *fre* while training the model with contrastive loss and cross-entropy loss separately. We find that contrastive loss helps in learning better feature representation and improving robustness under distributional shift, while the proposed query functions help in selecting unbiased and diverse samples that guides the contrastive loss to learn feature representations from the most informative samples. We observe CoreSet approach that performs well with cross-entropy loss, suffers when trained with contrastive loss resulting in higher sampling bias and lower accuracy. The results from our ablation studies on CIFAR10 and Imbalanced-CIFAR10 is provided in Appendix B.1. We empirically show combining contrastive loss and proposed query functions (*featuresim* and *fre*) together benefits in active learning setting for imbalanced and balanced datasets.

## 5 Conclusion

We introduced supervised contrastive active learning by proposing computationally inexpensive but efficient query methods to select diverse and informative data samples in active learning, achieving state-of-the-art accuracy in both imbalanced and balanced dataset setup. The proposed methods yield good model calibration next to Bayesian active learning by disagreement, with a significantly lesser query time for sample acquisition. We compared the robustness to distributional shift of models derived from various state-of-the-art query methods in the active learning setting. The supervised contrastive active learning outperforms other high-performing methods by a big margin in robustness to dataset shift and out-of-distribution. Further, our query strategy reduces sampling bias from both balanced and imbalanced datasets. We envision the proposed active learning method can help in building efficient, robust, fair and trustworthy models.

## References

- Ahuja, N. A.; Ndiour, I.; Kalyanpur, T.; and Tickoo, O. 2019. Probabilistic modeling of deep features for out-of-distribution and adversarial detection. *arXiv preprint arXiv:1909.11786*.
- Beluch, W. H.; Genewein, T.; Nürnberger, A.; and Köhler, J. M. 2018. The power of ensembles for active learning in image classification. In *Proceedings of the IEEE Conference on Computer Vision and Pattern Recognition*, 9368–9377.
- Bhatt, U.; Antorán, J.; Zhang, Y.; Liao, Q. V.; Sattigeri, P.; Fogliato, R.; Melançon, G. G.; Krishnan, R.; Stanley, J.; Tickoo, O.; et al. 2021. Uncertainty as a form of transparency: Measuring, communicating, and using uncertainty. *AAAI/ACM Conference on Artificial Intelligence, Ethics, and Society (AIES)*.
- Blundell, C.; Cornebise, J.; Kavukcuoglu, K.; and Wierstra, D. 2015. Weight Uncertainty in Neural Network. In *International Conference on Machine Learning*, 1613–1622.
- Brier, G. W. 1950. Verification of forecasts expressed in terms of probability. *Monthly weather review*, 78(1): 1–3.
- Brinker, K. 2003. Incorporating diversity in active learning with support vector machines. In *Proceedings of the 20th international conference on machine learning (ICML-03)*, 59–66.
- Buolamwini, J.; and Gebru, T. 2018. Gender shades: Intersectional accuracy disparities in commercial gender classification. In *Conference on fairness, accountability and transparency*, 77–91. PMLR.
- Cao, K.; Wei, C.; Gaidon, A.; Arechiga, N.; and Ma, T. 2019. Learning Imbalanced Datasets with Label-Distribution-Aware Margin Loss. *Advances in Neural Information Processing Systems*, 32: 1567–1578.
- Chen, T.; Kornblith, S.; Norouzi, M.; and Hinton, G. 2020a. A simple framework for contrastive learning of visual representations. In *International conference on machine learning*, 1597–1607. PMLR.
- Chen, T.; Kornblith, S.; Swersky, K.; Norouzi, M.; and Hinton, G. 2020b. Big Self-Supervised Models are Strong Semi-Supervised Learners. *arXiv preprint arXiv:2006.10029*.
- Chen, X.; Fan, H.; Girshick, R.; and He, K. 2020c. Improved baselines with momentum contrastive learning. *arXiv preprint arXiv:2003.04297*.
- Cordts, M.; Omran, M.; Ramos, S.; Rehfeld, T.; Enzweiler, M.; Benenson, R.; Franke, U.; Roth, S.; and Schiele, B. 2016. The cityscapes dataset for semantic urban scene understanding. In *Proceedings of the IEEE conference on computer vision and pattern recognition*, 3213–3223.
- Dasgupta, S. 2011. Two faces of active learning. *Theoretical computer science*, 412(19): 1767–1781.
- Dasgupta, S.; and Hsu, D. 2008. Hierarchical sampling for active learning. In *Proceedings of the 25th international conference on Machine learning*, 208–215.
- Davis, J.; and Goadrich, M. 2006. The relationship between Precision-Recall and ROC curves. In *Proceedings of the 23rd international conference on Machine learning*, 233–240.
- Ducoffe, M.; and Precioso, F. 2018. Adversarial active learning for deep networks: a margin based approach. *Proceedings of the 35th International Conference on Machine Learning*.
- Farquhar, S.; Gal, Y.; and Rainforth, T. 2020. On Statistical Bias In Active Learning: How and When to Fix It. In *International Conference on Learning Representations*.
- Gal, Y.; and Ghahramani, Z. 2016. Dropout as a bayesian approximation: Representing model uncertainty in deep learning. In *international conference on machine learning*, 1050–1059. PMLR.
- Gal, Y.; Islam, R.; and Ghahramani, Z. 2017. Deep bayesian active learning with image data. In *International Conference on Machine Learning*, 1183–1192. PMLR.
- Gneiting, T.; and Raftery, A. E. 2007. Strictly proper scoring rules, prediction, and estimation. *Journal of the American statistical Association*, 102(477): 359–378.
- He, K.; Fan, H.; Wu, Y.; Xie, S.; and Girshick, R. 2020. Momentum contrast for unsupervised visual representation learning. In *Proceedings of the IEEE/CVF Conference on Computer Vision and Pattern Recognition*, 9729–9738.
- He, K.; Zhang, X.; Ren, S.; and Sun, J. 2016. Deep residual learning for image recognition. In *Proceedings of the IEEE conference on computer vision and pattern recognition*, 770–778.
- Hendrycks, D.; and Dietterich, T. 2018. Benchmarking Neural Network Robustness to Common Corruptions and Perturbations. In *International Conference on Learning Representations*.
- Hendrycks, D.; and Gimpel, K. 2017. A Baseline for Detecting Misclassified and Out-of-Distribution Examples in Neural Networks. *Proceedings of International Conference on Learning Representations*.
- Houlsby, N.; Huszár, F.; Ghahramani, Z.; and Lengyel, M. 2011. Bayesian active learning for classification and preference learning. *arXiv preprint arXiv:1112.5745*.
- Irvin, J.; Rajpurkar, P.; Ko, M.; Yu, Y.; Ciurea-Ilicus, S.; Chute, C.; Marklund, H.; Haghgoo, B.; Ball, R.; Shpanskaya, K.; et al. 2019. Chexpert: A large chest radiograph dataset with uncertainty labels and expert comparison. In *Proceedings of the AAAI Conference on Artificial Intelligence*, volume 33, 590–597.
- Khosla, P.; Teterwak, P.; Wang, C.; Sarna, A.; Tian, Y.; Isola, P.; Maschinot, A.; Liu, C.; and Krishnan, D. 2020. Supervised Contrastive Learning. In *Advances in Neural Information Processing Systems*, volume 33, 18661–18673.
- Kirsch, A.; Van Amersfoort, J.; and Gal, Y. 2019. Batchbald: Efficient and diverse batch acquisition for deep bayesian active learning. *Advances in neural information processing systems*, 32: 7026–7037.
- Krishnan, R.; and Tickoo, O. 2020. Improving model calibration with accuracy versus uncertainty optimization. *Advances in Neural Information Processing Systems*, 33.
- Krizhevsky, A.; et al. 2009. Learning multiple layers of features from tiny images.
- Lewis, D. D.; and Gale, W. A. 1994. A sequential algorithm for training text classifiers. In *SIGIR '94*, 3–12. Springer.

Liu, Z.; Miao, Z.; Zhan, X.; Wang, J.; Gong, B.; and Yu, S. X. 2019. Large-scale long-tailed recognition in an open world. In *Proceedings of the IEEE/CVF Conference on Computer Vision and Pattern Recognition*, 2537–2546.

Naeini, M. P.; Cooper, G.; and Hauskrecht, M. 2015. Obtaining well calibrated probabilities using bayesian binning. In *Twenty-Ninth AAAI Conference on Artificial Intelligence*.

Netzer, Y.; Wang, T.; Coates, A.; Bissacco, A.; Wu, B.; and Ng, A. Y. 2011. Reading digits in natural images with unsupervised feature learning.

Ovadia, Y.; Fertig, E.; Ren, J.; Nado, Z.; Sculley, D.; Nowozin, S.; Dillon, J.; Lakshminarayanan, B.; and Snoek, J. 2019. Can you trust your model's uncertainty? Evaluating predictive uncertainty under dataset shift. In *Advances in Neural Information Processing Systems*, volume 32.

Paszke, A.; Gross, S.; Massa, F.; Lerer, A.; Bradbury, J.; Chanan, G.; Killeen, T.; Lin, Z.; Gimelshein, N.; Antiga, L.; Desmaison, A.; Kopf, A.; Yang, E.; DeVito, Z.; Raison, M.; Tejani, A.; Chilamkurthy, S.; Steiner, B.; Fang, L.; Bai, J.; and Chintala, S. 2019. PyTorch: An Imperative Style, High-Performance Deep Learning Library. In *Advances in Neural Information Processing Systems*, volume 32.

Quionero-Candela, J.; Sugiyama, M.; Schwaighofer, A.; and Lawrence, N. D. 2009. *Dataset shift in machine learning*. The MIT Press.

Sener, O.; and Savarese, S. 2018. Active Learning for Convolutional Neural Networks: A Core-Set Approach. In *International Conference on Learning Representations*.

Settles, B. 2009. Active learning literature survey.

Shannon, C. E. 1948. A mathematical theory of communication. *Bell system technical journal*, 27(3): 379–423.

Shen, Y.; Yun, H.; Lipton, Z. C.; Kronrod, Y.; and Anandkumar, A. 2018. Deep Active Learning for Named Entity Recognition. In *International Conference on Learning Representations*.

Shui, C.; Zhou, F.; Gagné, C.; and Wang, B. 2020. Deep active learning: Unified and principled method for query and training. In *International Conference on Artificial Intelligence and Statistics*, 1308–1318. PMLR.

Tack, J.; Mo, S.; Jeong, J.; and Shin, J. 2020. CSI: Novelty Detection via Contrastive Learning on Distributionally Shifted Instances. *Advances in Neural Information Processing Systems*, 33: 11839–11852.

Tong, S.; and Koller, D. 2001. Support vector machine active learning with applications to text classification. *Journal of machine learning research*, 2(Nov): 45–66.

Van der Maaten, L.; and Hinton, G. 2008. Visualizing data using t-SNE. *Journal of machine learning research*, 9(11).

Yoo, D.; and Kweon, I. S. 2019. Learning loss for active learning. In *Proceedings of the IEEE/CVF Conference on Computer Vision and Pattern Recognition*, 93–102.

Zhang, R.; Li, C.; Zhang, J.; Chen, C.; and Wilson, A. G. 2019. Cyclical Stochastic Gradient MCMC for Bayesian Deep Learning. In *International Conference on Learning Representations*.

## Appendix

### A Experimental details

#### A.1 Datasets

- **CIFAR-10** (Krizhevsky et al. 2009): This dataset consists training set of 50,000 examples and a test set of 10,000 examples. Each example is a 32x32 RGB color image, associated with a label from 10 classes. CIFAR-10 is a balanced dataset with 5000 examples and 1000 examples from each class in training and test set respectively. In our setup, we consider the 50,000 examples part of the unlabelled pool and evaluate the model with 10,000 test examples at every iteration of the active learning cycle.
- **Imbalanced-CIFAR10** (Cao et al. 2019): Long-tailed version of CIFAR10 is created following an exponential decay in sample sizes across different classes. The imbalance ratio is set to 50, the ratio of sample size in most frequent class to the sample size in least frequent class. The long-tailed Imbalanced-CIFAR10 dataset with imbalance ratio  $\rho = 50$  has 13996 train samples with the number of samples in each class include: [5000, 3237, 2096, 1357, 878, 568, 368, 238, 154, 100]. This long-tailed data is used as unlabelled set to train models with active learning. The test set has balanced 10,000 samples.
- **SVHN** (Netzer et al. 2011): The Street View House Numbers (SVHN) dataset has house numbers obtained from Google Street View images to recognize the digits (0-9, representing 10 classes). The dataset has 73257 training and 26032 test images. The images are 32x32 color image patches centered around a single digit. In our setup, we consider the 73257 examples part of the unlabelled pool and evaluate the model with 10,000 test examples at every iteration of the active learning cycle. SVHN dataset has class imbalance with the number of samples in each class include: [4948, 13861, 10585, 8497, 7458, 6882, 5727, 5595, 5045, 4659].
- **CIFAR10-C** (Hendrycks and Dietterich 2018): CIFAR10 test set (10,000 samples) corrupted with 16 different types of perturbations ('brightness', 'contrast', 'defocus blur', 'elastic transform', 'fog', 'frost', 'gaussian blur', 'gaussian noise', 'glass blur', 'impulse noise', 'pixelate', 'saturate', 'shot noise', 'spatter', 'speckle noise', 'zoom blur') and 5 different levels of intensities (1 to 5), totally 80 different variations of test set. We use this data to evaluate the robustness to dataset shift on models trained with clean CIFAR10.

#### A.2 Model details and hyperparameters

We use ResNet-18 (He et al. 2016) model architecture for all the methods and datasets under study. We use the same hyperparameters for all the models for a fair comparison. At each iteration in active learning, the models are trained with labeled samples acquired through the query strategy from respective methods. The models are trained with SGD optimizer for 200 epochs with an initial learning rate of 0.1, momentum of 0.9 and weight decay of 0.0005. As part of the learning rate schedule, the initial learning rate was multiplied by 0.1 at epoch 160. The training samples were augmented

with random horizontal flips and random crops for all the methods, an additional random grayscale with probability of 0.2 is used for SCAL as Contrastive loss relies on augmentation. At the end of each active learning iteration, the models were evaluated with the labeled test set. We used these hyperparameters for all three datasets in our experiments.

At every iteration  $n$  in the active learning, we obtain a random subset  $\mathcal{D}_S \subset \mathcal{D}_U^n$  of 10K samples from the remaining unlabeled sets for CIFAR10 and SVHN, from which  $M$  most informative samples are selected using query strategy. This subset strategy in the unlabeled pool has been suggested in (Beluch et al. 2018; Yoo and Kweon 2019) to avoid picking overlapping similar samples. The subset size is set to 8000 for Imbalanced-CIFAR10 as the number of data samples available in the unlabeled pool is lower (13.9k samples). At every iteration, we choose and annotate  $M = 1000$  (for CIFAR10 and SVHN datasets) and  $M = 500$  (for Imbalanced-CIFAR10) additional samples according to the strategy described in Section 3.

#### A.3 Implementation details

We implemented the models and methods including SCAL (featuresim), SCAL (fre), BALD, Entropy and Random for our experiments using PyTorch (Paszke et al. 2019) framework. The experiments for CoreSet (Sener and Savarese 2018) and Learning loss (Yoo and Kweon 2019) methods are performed in PyTorch based on the open-source implementations<sup>†,‡</sup>.

The projection head and classifier for the SCAL method follow the same methodology as in (Khosla et al. 2020). The temperature parameter  $T$  was set to 0.07 in the contrastive loss. The scores are computed from the features of ResNet-18 network from the layer before last fully-connected layer.

BALD method is implemented with Monte-Carlo (MC) dropout (Gal and Ghahramani 2016) by introducing a dropout layer with probability of 0.3 after convolutional layers in the ResNet blocks. 50 stochastic forward passes are performed with dropout enabled during inference. We selected number of MC runs to be 50 in BALD method as the expected calibration error and accuracy saturated beyond 50 MC runs in our ablation study shown in Figure F15.

We report the results from 5 independent trials for each method at every active learning iteration.

#### A.4 Query strategy

- **Random**: Choose a random set of samples from unlabeled pool of data.
- **Entropy**: Choose a set of samples from an unlabeled pool that yields higher predictive entropy (Shannon 1948)

$$\mathcal{H}[y|x, D_L] := - \sum_{k=1}^K p(y = c_k|x, D_L) \log(p(y = c_k|x, D_L)) \quad (6)$$

- **CoreSet** (Sener and Savarese 2018): Choose the samples such that a model learned over the subset is competitive over the whole dataset. The query function selects points

<sup>†</sup> [https://github.com/google/active-learning/blob/master/sampling\\_methods/kcenter\\_greedy.py](https://github.com/google/active-learning/blob/master/sampling_methods/kcenter_greedy.py)

<sup>‡</sup> <https://github.com/Mephisto405/Learning-Loss-for-Active-Learning>

that minimizes the maximum Euclidean distance of any point to a center using k-Center-Greedy algorithm.

- **Learning Loss** (Yoo and Kweon 2019): Choose a set of samples based on the loss prediction module.
- **BALD** (Bayesian Active Learning by Disagreement) (Houlsby et al. 2011; Gal, Islam, and Ghahramani 2017): Choose a set of samples from an unlabeled pool that yields higher model uncertainty. Monte Carlo dropout (Gal and Ghahramani 2016) based Bayesian neural network is used to obtain model uncertainty for the unlabeled samples. The model uncertainty is quantified by the mutual information between the posterior distribution of weights and predictive distribution as defined in Equation (7). BALD can be implemented with other robust Bayesian neural network approximate inference methods such as variational inference (Blundell et al. 2015) and stochastic gradient MCMC (Zhang et al. 2019) to get well-calibrated uncertainty estimates, but we are not studying them in this paper.

$$\mathcal{I}[y, w | x, \mathcal{D}_L] := \mathcal{H}[y | x, \mathcal{D}_L] - \mathbb{E}_{p(w|\mathcal{D}_L)}[\mathcal{H}[p(y | x, w)]] \quad (7)$$

- **SCAL (*featuresim*)** and **SCAL (*fre*)**: The sample selection strategy for our proposed methods is described in Section 3.1.

## B Additional Results

### B.1 Ablation study: Effect of different query methods and loss functions

We performed ablation study to understand the effect of proposed query functions *featuresim* and *fre*, and training the model with contrastive versus cross-entropy loss in active learning setting. We compared the query methods including Random, Entropy, CoreSet, *featuresim* and *fre* while training the model with contrastive loss and cross-entropy loss separately. We performed these ablation studies on CIFAR10 and Imbalanced-CIFAR10 datasets.

We find that contrastive loss helps in learning better feature representation and improving robustness under distributional shift, while the proposed query functions help in selecting unbiased and diverse samples that guides the contrastive loss to learn feature representations from the most informative samples. Figures F1-(c), F2-(c), F3-(c) and F4-(c) show that the proposed sample selection scoring functions *featuresim* and *fre* helps in reducing the sampling bias while learning from both balanced and imbalanced datasets, irrespective of contrastive or cross-entropy loss. Fig. F1-(d) and Fig. F2-(d) show that contrastive loss helps in improved robustness to distributional shift (higher AUROC for out-of-distribution detection). We observe CoreSet approach that performs well with cross-entropy loss, suffers when trained with contrastive loss resulting in higher sampling bias (as seen in Fig. F1-(c) and Fig. F3-(c)) and lower accuracy (as seen in Fig. F1-(a) and Fig. F3-(a)). Figures F1-(a),(b) and F3-(a),(b) show combining the contrastive loss and query functions *featuresim/fre* benefits in active learning setting

for imbalanced and balanced datasets, supporting the results presented in Section 4.3.

### B.2 Qualitative analysis using tSNE (t-distributed Stochastic Neighbor Embedding)

We study the feature representations obtained from different methods with t-SNE (Van der Maaten and Hinton 2008) embeddings. Figures F5-F8 show the feature embeddings from different methods and sample selection exploration in active learning. The plots visualize the data samples corresponding to 10 classes with 10 different colors and the selected data with black markers, which is considered as most informative samples by the query strategies of corresponding methods. We notice that the features of SCAL method is well clustered even in the initial iterations of active learning as compared to other methods, this justifies the higher accuracy and lower expected calibration error for SCAL.

We further investigate the superior performance of SCAL under dataset shift (Fig. 5) with t-SNE embeddings. We compute the feature embeddings for the shifted data (CIFAR-10 corrupted with Gaussian Blur (Hendrycks and Dietterich 2018)) at each active learning iteration after the models are trained with clean labeled set. Figures F9-F12 show the feature embeddings of SCAL method is well clustered and well separated between classes even under dataset shift, as compared to other methods.

### B.3 Model calibration and reliability

In addition to Expected Calibration Error (ECE) (Naeini, Cooper, and Hauskrecht 2015) presented in Fig. 4, we evaluate model calibration and robustness using Brier score (Brier 1950). Fig. F13 compares the active learning methods on Imbalanced-CIFAR10, CIFAR10 and CIFAR10-C with Brier score, which is a proper scoring rule (Gneiting and Raftery 2007) for evaluating the model calibration. We present the results with (1+Brier) for easier readability. Fig. F14 show the comparison under dataset shift at different intensity levels.

### B.4 Model accuracy when trained with full dataset

The test accuracy when the model is trained using entire training set with cross entropy (Imbalanced-CIFAR10: 79.53%, CIFAR10: 93.04%, SVHN: 95.93%), or contrastive (Imbalanced-CIFAR10: 79.36%, CIFAR10: 92.69%, SVHN: 95.54%) loss indicates the upper bound on the accuracy that can be achieved in active learning setting without labeling 100% of training set. The results are provided in Appendix Table 3.

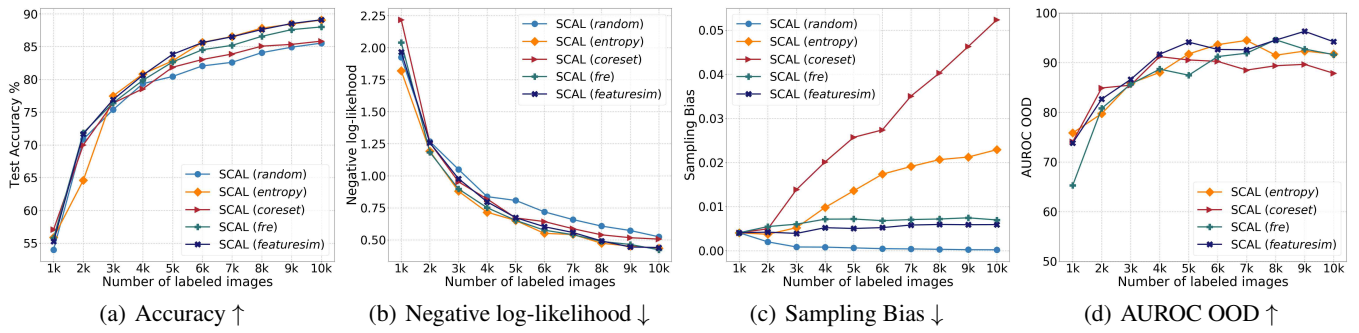


Figure F1: CIFAR10/ResNet-18: Ablation study of different query functions in active learning with models trained with **contrastive loss**

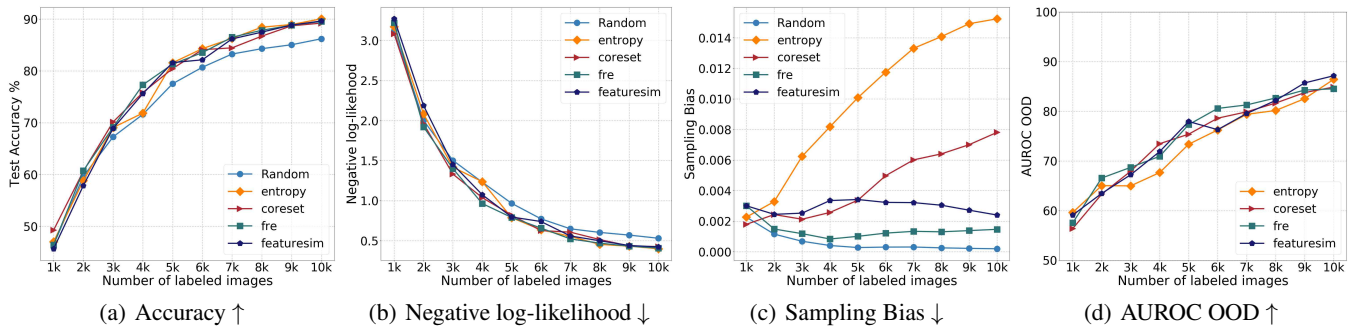


Figure F2: CIFAR10/ResNet-18: Ablation study of different query functions in active learning with models trained with **cross-entropy loss**

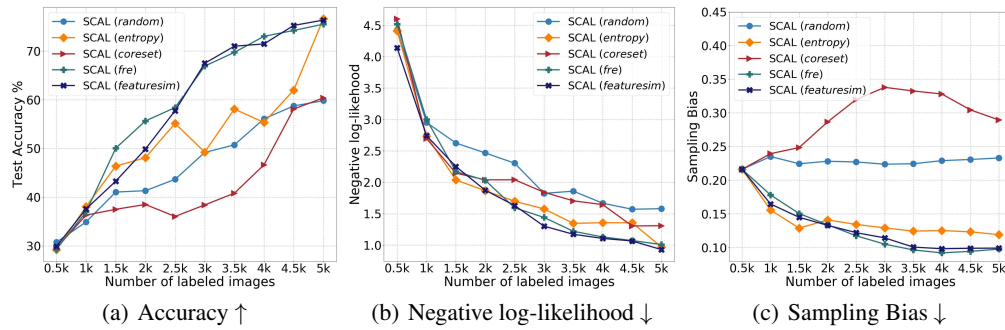


Figure F3: Imbalanced-CIFAR10/ResNet-18: Ablation study of different query functions with models trained with **contrastive loss**

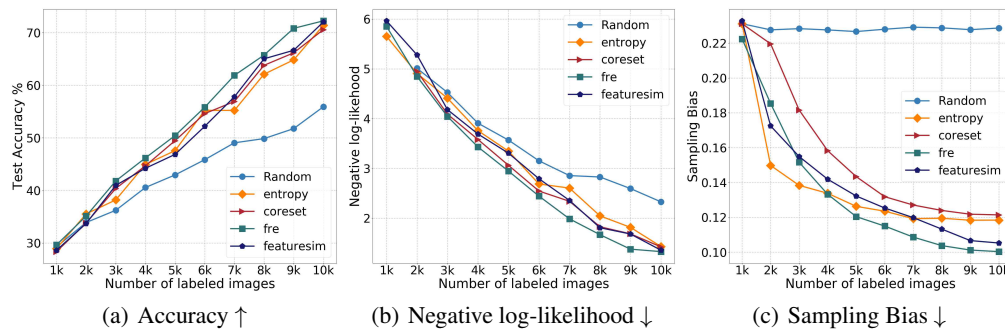


Figure F4: Imbalanced-CIFAR10/ResNet-18: Ablation study of different query functions with models trained with **cross-entropy loss**

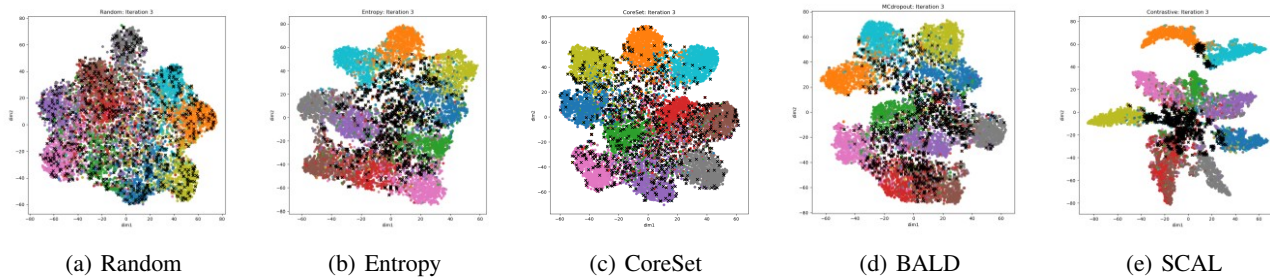


Figure F5: Active learning Iteration 3: tSNE plots for CIFAR-10/ResNet-18

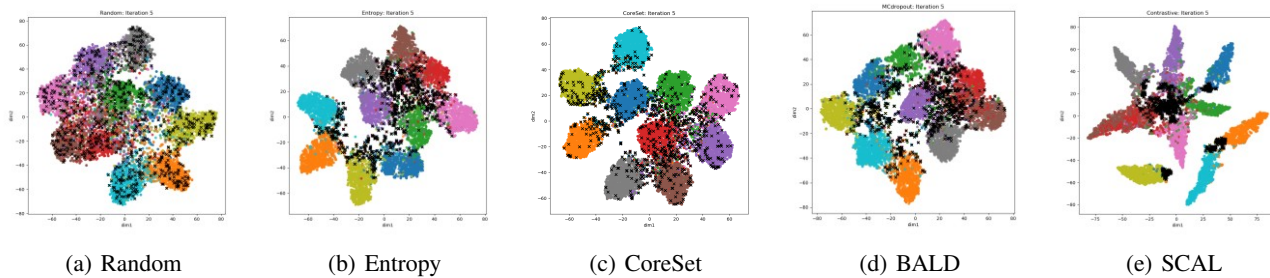


Figure F6: Active learning Iteration 5: tSNE plots for CIFAR-10/ResNet-18

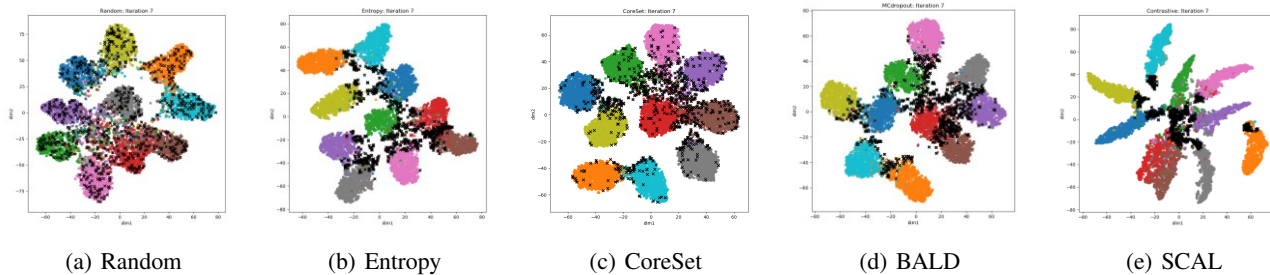


Figure F7: Active learning Iteration 7: tSNE plots for CIFAR-10/ResNet-18

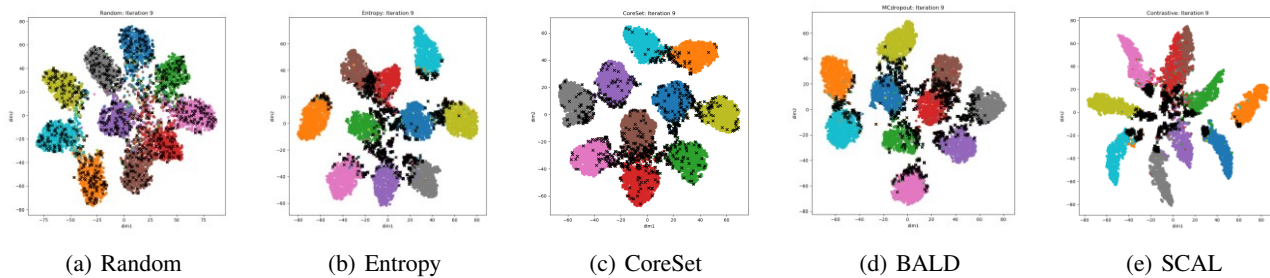


Figure F8: Active learning Iteration 9: tSNE plots for CIFAR-10/ResNet-18

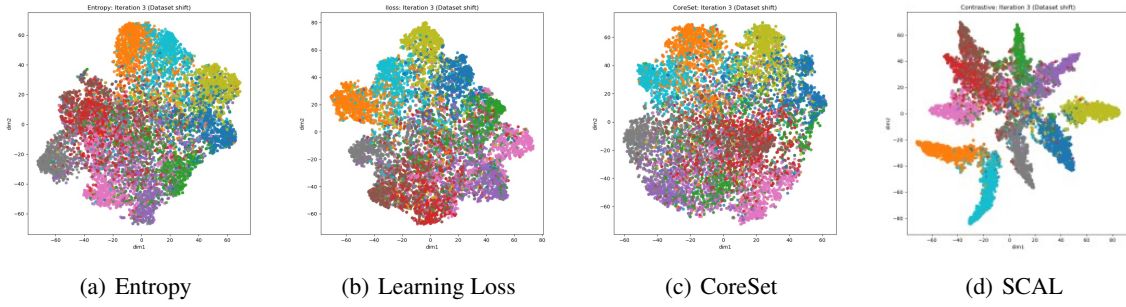


Figure F9: tSNE plots for dataset shift (CIFAR10 corrupted with Gaussian blur) - Active learning Iteration 3

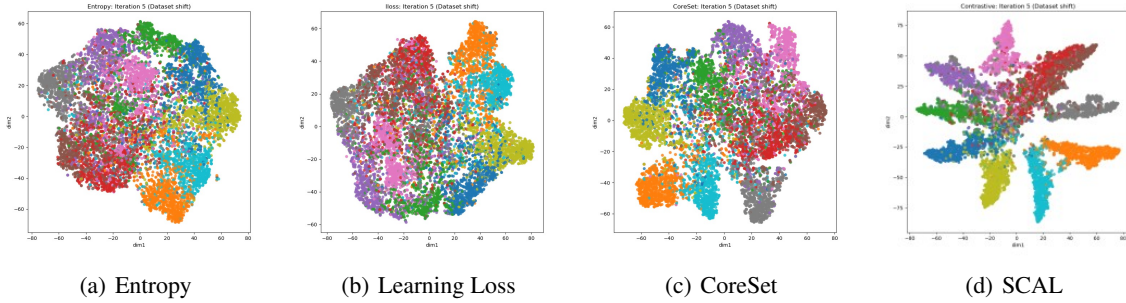


Figure F10: tSNE plots for dataset shift (CIFAR10 corrupted with Gaussian blur) - Active learning Iteration 5

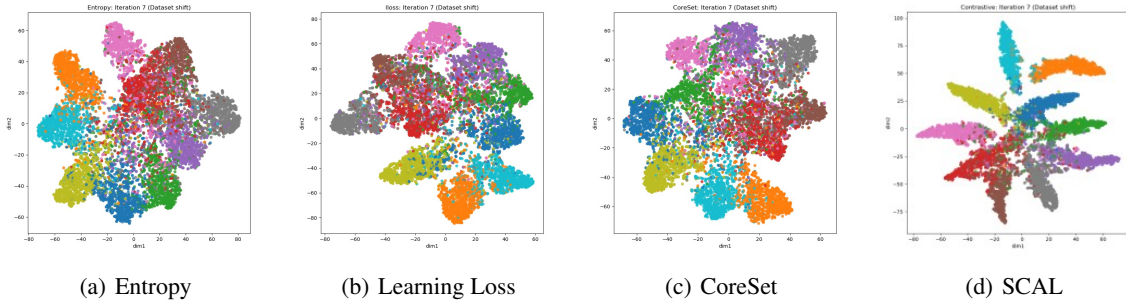


Figure F11: tSNE plots for dataset shift (CIFAR10 corrupted with Gaussian blur) - Active learning Iteration 7

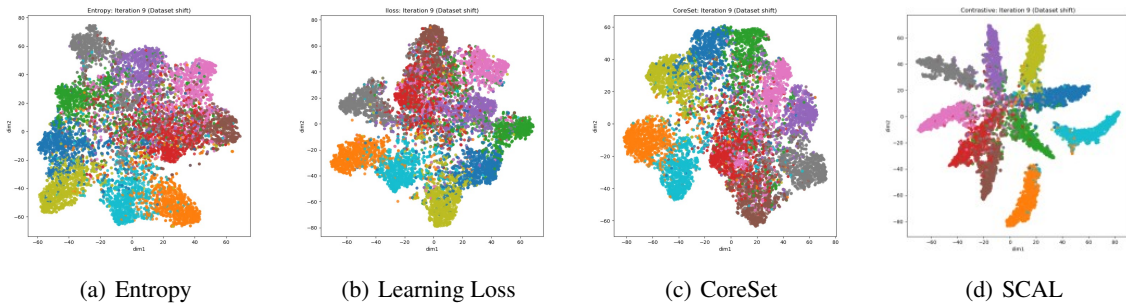


Figure F12: tSNE plots for dataset shift (CIFAR10 corrupted with Gaussian blur) - Active learning Iteration 9

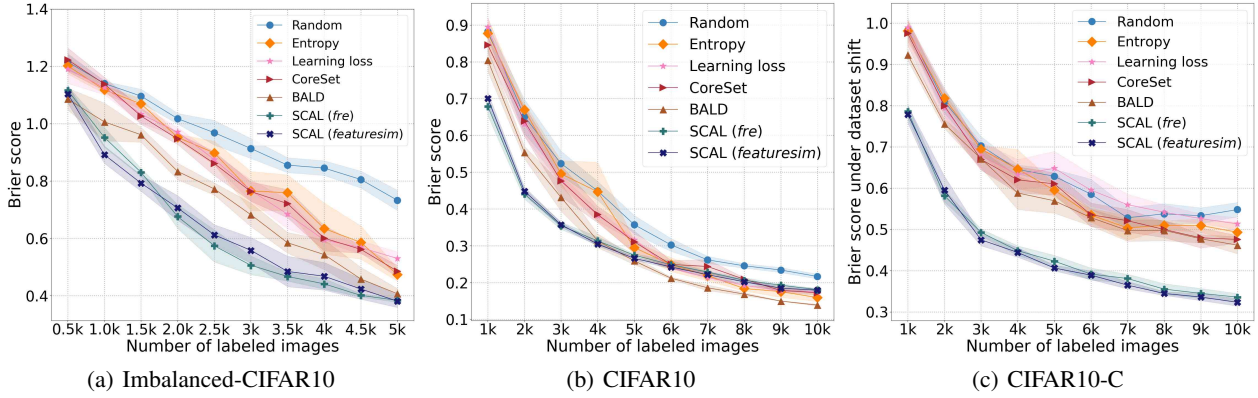


Figure F13: Brier score (lower is better) evaluation of different query methods on Imbalanced-CIFAR10, CIFAR10 and CIFAR10-C datasets in active learning. The shading shows std-dev from 5 independent trials for each method. We present the results as (1+Brier) for easier readability. Lower Brier score indicates the model is well-calibrated.

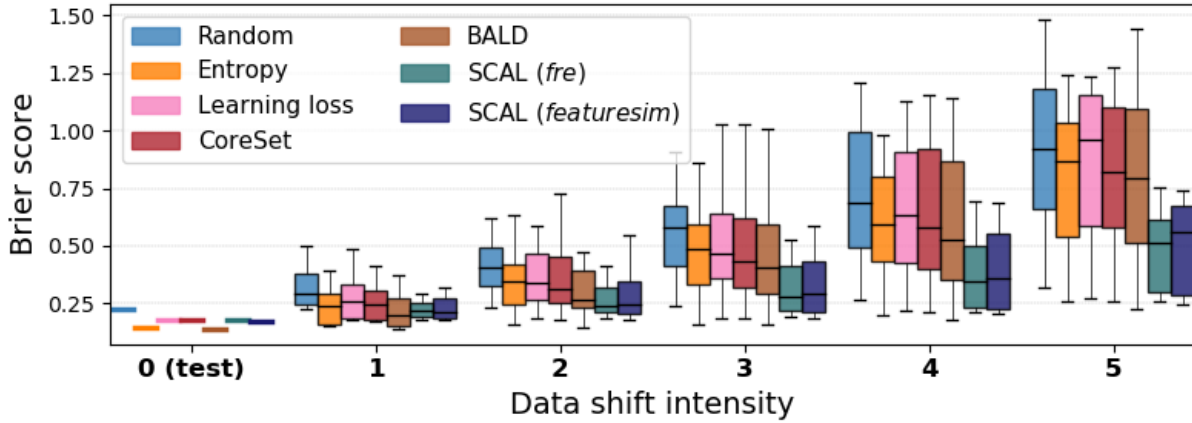
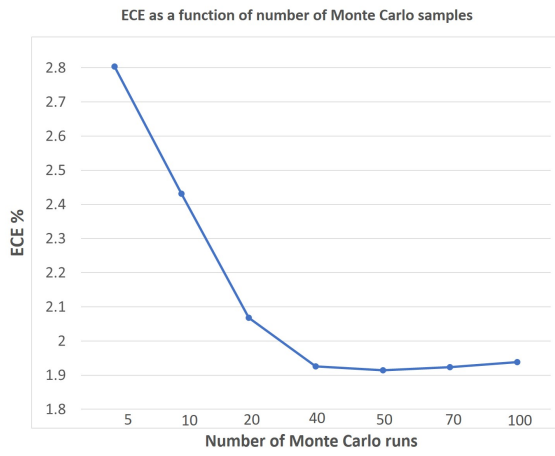


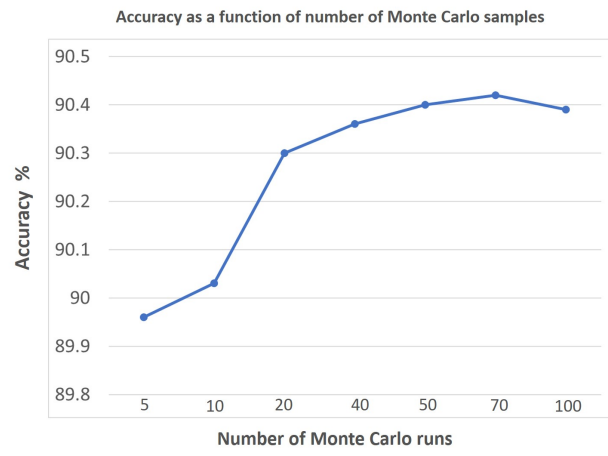
Figure F14: Brier score (lower is better) under dataset shift. Comparison of models derived with different query methods in active learning setting (10th iteration). At each shift intensity level, the boxplot summarizes the Brier score across 16 different datashift types showing the min, max and quartiles. Our proposed **SCAL** consistently yields lower Brier score even under increased dataset shift intensity, demonstrating better robustness compared to other state-of-the-art methods.

Table 3: Test accuracy (Test Acc) for training with different loss functions using the entire dataset. This table indicates an upper bound on the achievable accuracy.

DATASET	LOSS FUNCTION	# OF TRAIN SAMP	TEST ACC (%)
IMBALANCED-CIFAR 10	CROSSENTROPY	13996	79.53
	CROSSENTROPY+DROPOUT	13996	78.51
	CONTRASTIVE	13996	79.36
CIFAR10	CROSSENTROPY	50000	93.04
	CROSSENTROPY+DROPOUT	50000	92.23
	CONTRASTIVE	50000	92.69
SVHN	CROSSENTROPY	73257	95.93
	CROSSENTROPY+DROPOUT	73257	95.54
	CONTRASTIVE	73257	96.06



(a) ECE ↓



(b) Accuracy ↑

Figure F15: Ablation study (BALD): Accuracy and ECE as a function of number of Monte Carlo runs in BALD method (MC Dropout)